Received: 5 October 2020 | Accepted: 8 February 2021

DOI: 10.1111/ppa.13362

Plant Pathology WILEY

ORIGINAL ARTICLE

A statistical protocol to describe differences among nutrient utilization patterns of *Fusarium* spp. and *Trichoderma gamsii*

Giovanna Jona Lasinio[1] | Alessio Pollice[2] | Livia Pappalettere[3] | Giovanni Vannacci[3] | Sabrina Sarrocco[3]

[1]Department of Statistical Sciences, "Sapienza" University of Rome, Rome, Italy

[2]Department of Economics and Finance, University of Bari Aldo Moro, Largo Abbazia Santa Scolastica, Bari, Italy

[3]Department of Agriculture, Food and Environment, University of Pisa, Pisa, Italy

Correspondence
Sabrina Sarrocco, Department of Agriculture, Food and Environment, University of Pisa, Via del Borghetto 80, 56124 Pisa, Italy.
Email: sabrina.sarrocco@unipi.it

Alessio Pollice, Department of Economics and Finance, Univeristy of Bari Aldo Moro, Largo Abbazia Santa Scolastica, Bari, Italy.
Email: alessio.pollice@uniba.it

Abstract

The Biolog phenotype microarrays (PM) system offers a simple and cheap tool to rapidly provide a high throughput of information about the phenotypes of fungal isolates in a short time. In order to improve the use of the PM system in fungal ecology studies, the present work proposes a new statistical protocol based on two approaches, that is, a functional principal components analysis to describe similarity patterns of growth curves, and a Bayesian generalized additive model (GAM) to allow inferences on specific growth features, in order to analyse nutrient fungal utilization in a model system including four causal agents of Fusarium head blight, the natural competitor *Fusarium oxysporum*, and the beneficial isolate *Trichoderma gamsii* T6085. Analysis of data collected by the Biolog PM in our biological system showed a different nutritional competitive potential of the four pathogens, as well as an intermediate behaviour of the natural competitor and of our biocontrol agent. This protocol, applicable to different fungal phenotypical studies at both isolate and community level, allows a full exploitation of data obtained by the PM system and provides important information about the nutritional pattern of a single isolate compared to those of other fungi, a key factor to be exploited in biocontrol strategies.

KEYWORDS
Bayesian generalized additive models, Biolog phenotype microarray system, functional clustering, fungal nutrient utilization, Fusarium head blight

1 | INTRODUCTION

Within an ecological community, populations can interact directly and indirectly either in an intraspecific (between individuals of the same species) or interspecific (between two or more species) way (Brooker et al., 2009). Interspecific competition occurs when there is the simultaneous demand for the same resource that is in limiting supply, that is, not enough to meet the demands for all involved species. Two competition strategies generally occur within fungal communities: interference competition—monopolization of the habitat by antagonistic combat (Sarrocco, 2016); and exploitation competition—when one organism, by exploiting the resource, reduces its availability to another organism with no physical interaction between them (Holomuzki et al., 2010). Competition is an important threat in plant pathology. Intra- and interspecific competition among pathogens can occur across space and time when spatial niche differentiation and/or temporal separation fail (Fitt et al., 2006). In addition, competitive interaction within a coexisting population is one of the mechanisms to control plant disease and to reduce pathogen populations (Kinkel et al., 2014). An example of a disease where nutrient competition plays a crucial role for the survival and development of the causal agents is Fusarium head blight (FHB) of small grain cereals. FHB, recognized as one of the most serious problems affecting wheat all over the world, is caused by a complex of around 20 fungal species, mostly belonging to *Fusarium* genus. Within this group,

F. graminearum species complex (FGSC), as well as *F. avenaceum*, *F. culmorum*, and *F. poae*, are considered as the major species. From the perspective of the global incidence of this disease, other species such as *F. acuminatum*, *F. cerealis*, *F. chlamydosporum*, *F. equiseti*, *F. langsethiae*, *F. sporotrichioides*, and *F. tricinctum* are considered less important (Torres et al., 2019). From an ecological point of view, FHB causal agents seem to interact in a competitive rather than in a synergistic way during pathogen/disease development (Xu & Nicholson, 2009).

During the disease cycle, plant debris is used by the pathogens to overwinter between two following cropping seasons, while spikes at flowering are the most susceptible stage of wheat to infection. Application of beneficial fungi on cultural debris, as well as on spikes during anthesis, is based on the efficacy of competition for space and nutrients as a mechanism to control FHB causal agents (Sarrocco et al., 2019; Sarrocco & Vannacci, 2018).

The knowledge of the nutritional requirements of fungi potentially involved in competitive relationships with pathogens is of great interest in view of a future application in the field. The Biolog phenotype microarray (PM) system represents a valid, simple to use, and relatively cheap tool to rapidly investigate niche overlap and catabolic versatility of fungi by testing isolates against many different carbon sources one at a time (Pinzari et al., 2016). Until now, data collected by Biolog analysis, consisting of the spectrophotometric reads at regular intervals of the multiwell plates (95 wells containing different substrates plus one control well containing water), have been analysed by different approaches. These include common analysis of single time-point optical density values across substrates at a given reading point, as well as in model-based approaches developed in order to describe the kinetics of carbon source utilization by fungi (Wirsel et al., 2002). Empirical models—in particular, semiparametric regression splines—have now been implemented to extrapolate growth curve parameters such as lag time, maximum rate of increase, and maximum optical density (Vaas et al., 2012). In general, data analysis is still a very controversial and complex aspect of using Biolog for fungal ecological studies.

In order to improve the use of the Biolog system in fungal phenotyping studies, the present work proposes a statistical protocol to analyse nutrient utilization in fungi based on all the information included in each growth curve on all the substrates, by using—as a model system—four causal agents of FHB, a natural fungal competitor against these pathogens (*Fusarium oxysporum*), and a well-known beneficial isolate of *Trichoderma gamsii* (T6085) showing promising capabilities for use as a biocontrol agent for the management of FHB disease.

2 | MATERIALS AND METHODS

2.1 | Fungal isolates

T. gamsii T6085 was isolated in Crimea (Ukraine) from uncultivated soil and has been studied over a long period of time for its ability to control *F. graminearum*, one of the main causal agents of FHB on wheat (Baroncelli et al., 2016; Matarese et al., 2012). *F. oxysporum* 7121 belongs to a wider collection of *F. oxysporum* strains isolated from wheat straw buried in soils collected close to Pisa (Italy) with a previous history of wheat cultivation. This isolate was selected because it is able to grow in the presence of 50 ppm deoxynivalenol (DON) and for its ability to colonize natural substrates (Sarrocco et al., 2019).

F. graminearum ITEM 124 was isolated from *Oryza sativa* in Italy and its genome was recently sequenced, annotated, and released (Zapparata et al., 2017). *F. culmorum* ITEM 627 was isolated from *Triticum durum* in former Yugoslavia, while *F. langsethiae* ITEM 11031 was isolated from *Zea mays* in Italy. *F. graminearum*, *F. culmorum*, and *F. langsethiae* were kindly given by Antonio Moretti (ISPA-CNR, Bari, Italy; http://www.ispa.cnr.it/Collection). *F. sporotrichioides* 194, isolated from *T. durum* in Italy, was kindly given by Giovanni Beccari (Department of Agricultural, Food and Environmental Sciences, University of Perugia, Italy).

All fungi, deposited in the Fungal Collection of the Plant Pathology & Mycology Lab (DISAAA-a, University of Pisa), were maintained on potato dextrose agar (PDA; Difco) under mineral oil at 4 °C for long-term storage and grown on PDA (*T. gamsii*, *F. oxysporum*, *F. culmorum*, *F. langsethiae*, and *F. sporotrichioides*) or oat meal agar (OA; Difco) (*F. graminearum*) at 24 °C, under a 12 hr light/dark photoperiod, when actively growing cultures were needed. All pathogenic *Fusarium* isolates were regularly inoculated on the host to maintain their virulence.

2.2 | Assessment of metabolic requirements

In order to set up a new statistical protocol to establish which substrates could potentially become a source of nutrient competition, the four pathogens belonging to the FHB complex, the natural competitor *F. oxysporum* 7121, and the potential biocontrol agent *T. gamsii* T6085 were analysed using the Biolog microbial identification system (https://www.biolog.com/products-portfolio-overview/microbial-identification/). A total of 100 μl of a water spore suspension (10^6 spores/ml) of each of the six fungal isolates was inoculated in each well of a Biolog multiwell plate (FF, for filamentous fungi, MicroPlate) containing water and 95 different carbon sources (https://www.biolog.com/wp-content/uploads/2020/04/00A-010rB-FF-Sell-Sheet-Mar07.pdf) and incubated at 24 °C with a 12 hr light/dark photoperiod. Two independent replicates were carried out for each isolate. Fungal growth was spectrophotometrically measured as optical density (OD) at 595 nm for 1 day, every 4 hr (12 hr during the night). The OD values, normalized against those for A1 (control well), were used in the present work to set up a new statistical protocol allowing a better exploitation of all the information contained within each fungal growth curve (created with OD values) on each substrate, as described in the following section.

2.3 | Statistical analysis protocol

A detailed analysis of fungal phenotypes based on specific nutrient utilization was obtained by a new statistical protocol (Figure 1) in order to

- cluster optical density growth curves into groups corresponding to relevant growth features (characterization), and
- compare and order fungal isolates within substrates according to relevant growth features (assessment).

We framed these two research questions into a preliminary exploratory (i.e., characterization in Figure 1) and a subsequent confirmatory (i.e., assessment in Figure 1) statistical environment and estimated the growth functions of the six isolates for all substrates by two approaches. To achieve the first target, growth curves of OD data for each isolate and substrate were projected onto an adequate basis, and curve clusters were found by functional clustering. To achieve the second, Bayesian growth predictions and credible intervals were obtained by semiparametric generalized additive models (GAMs) and were used to define and calculate the scores for each isolate on each substrate, while accounting for their uncertainty.

2.4 | Characterization – functional clustering

The main focus of conventional clustering algorithms is the definition of homogeneous subgroups of individuals in a data set. Cluster analysis is also often applied to longitudinal data, such as growth curves. In this case, a primary concern was to find curve patterns representing different shapes and variation. Recently, several clustering methods driven by the functional characteristics of the available data have been proposed. The common rationale is to project the observed growth curves to certain basis functions and to process curve projections by a functional mixed model.

In this work functional clustering (FC) was performed by the *k*-centres method described by Chiou and Li (2007) and implemented in the funcit function (Funcy R package v. 0.8.6; Yassouridis et al., 2018).

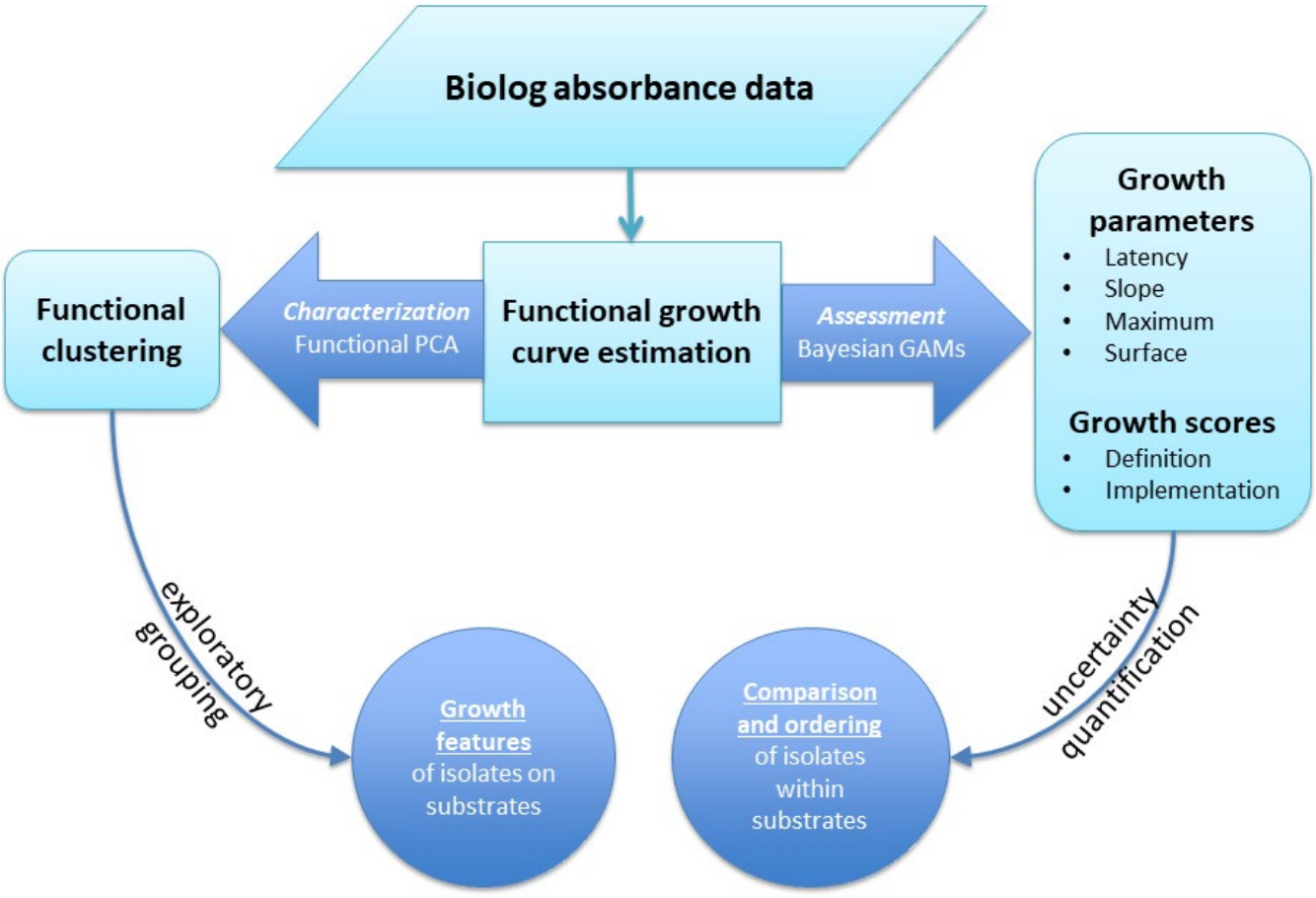

FIGURE 1 Analysis of fungal phenotypes based on nutrients utilization is obtained by exploratory clustering optical density growth curves into groups corresponding to growth features (characterization): growth curves of optical density(OD) data for each isolate and substrate are projected onto adequate basis and curve clusters are found by functional clustering; and confirmatory comparison and ordering fungal isolates within substrates according to growth features (assessment): Bayesian growth predictions and credible intervals are obtained by semiparametric generalized additive models (GAMs) and used to define and calculate scores for each isolate on each substrate, accounting for their uncertainty [Colour figure can be viewed at wileyonlinelibrary.com]

This method is a functional counterpart of the *k*-means algorithm as cluster membership is predicted with a reclassification step: alternately, curves are assigned to classes, and classes are calculated anew depending on their assigned curves. Each curve is projected into all *k* eigenspaces generated by functional principal component analysis and then it is assigned to one of them on the basis of a nonparametric random-effect model of the functional principal components, coupled with a nonparametric iterative mean and covariance updating scheme. Optical density growth data for each isolate and substrate were processed by the *k*-centres semiparametric FC method, with $k = 3$. According to cluster membership, each substrate was then classified as large (fast growth), medium (medium growth), or small (supporting poor growth).

2.5 | Assessment – Bayesian generalized additive models

The behaviour of each isolate in each substrate was assessed by an inferential procedure that allows a probabilistic comparison between isolate features within substrates. We first searched for the "best" estimate of each growth curve and then computed summary growth parameters describing the isolate behaviour within the substrates. We searched for the best model in the semiparametric class of GAMs. Let y_{ist} be the log-OD of the *i*-th isolate ($i = 1, \ldots, 6$) in substrate *s* ($s = 1, \ldots, 92$) at time x_t ($t = 1, \ldots, 17$, $x_t = 0, 4, \ldots, 96$) and assume it is expressed as follows:

$$y_{ist} = \mu_{is} + \beta_s x_t + f_s(x_t) + \beta_{is} x_t + f_{is}(x_t) + \varepsilon_{ist}$$

with μ_{is} average growth of isolate *i* in substrate *s*; β_s growth rate in substrate *s*; $f_s(x_t)$ nonlinear growth effect in substrate *s*; β_{is} growth rate of isolate *i* in substrate *s*; $f_{is}(x_t)$ nonlinear growth effect of isolate *i* in substrate *s*; ε_{ist} random error.

Generalized additive models are estimated in the Bayesian inferential framework making use of "spike and slab" prior distributions that allow a "stochastic search" selection of relevant model terms (Scheipl et al., 2012). In particular, this approach enables computation of the posterior inclusion probability of each model component (for each isolate within substrates). Then, the "best" model is obtained selecting model terms with large (>0.8) inclusion probabilities. Bayesian estimation is carried out using Monte Carlo simulations: for each growth curve we generated a collection of (100) simulated curves that can be seen as samples from the curve posterior probability distribution. These samples were used to build credible intervals for the growth curve as well as for any summary of the curve itself. In this work, 95% credible intervals were built using 0.025 and 0.975 percentiles of each curve (or summary parameter) distribution.

To summarize the growth features of each isolate in each substrate, we computed the following summary parameters:

- Latency λ
- Growth rate μ computed as the slope of the steepest tangent to the curve
- Maximum height A
- Surface under the curve S

For each parameter and fungal isolate we computed 95% credible intervals within substrates. Uncertainty measures were then used to define growth scores that allow comparison and ordering of isolates within substrates. Growth scores are obtained as follows: let p_{isk} be one of the four growth curve parameters for isolate $i = 1, \cdots, 6$, substrate $s = 1, \cdots, 93$ and $k = 1, \cdots, 4$ for latency λ, slope μ, maximum A, and surface S.

- Rescale all parameters to the range (0, 1) as follows: $\%p_{isk} = \frac{p_{isk} - \min_i(p_{isk})}{max_i(p_{isk}) - \min_i(p_{isk})}$
- Only for the latency parameter use $1 - \%\lambda_{isk}$ instead of $\%\lambda_{isk}$ to ease comparisons
- Consider, for example, the fungal pair (i, j)such that $\%p_{isk} > \%p_{jsk}$ in substrate *s*
- To define the partial scores of the *i*-th isolate within the *s*-th substrate for the *k*-th parameter check if the 95% credible intervals of $\%p_{isk}$ and $\%p_{jsk}$overlap
  a. YES → $SC_{isk} = SC_{jsk} = (\%p_{isk} + \%p_{jsk})/2$
  b. NO → $SC_{isk} = \%p_{isk}$ and $SC_{jsk} = -\%p_{jsk}$
- Define the average score of the *i*-th isolate within the *s*-th substrate as follows:

$$SC_{is} = \frac{1}{4}\sum_{k=1}^{4} SC_{isk}$$

3 | RESULTS

3.1 | Characterization – functional clustering

OD growth data for each isolate and substrate were processed by the *k*-centres semiparametric FC method, with $k = 3$. In Figure 2, growth curves for the six isolates on 93 substrates (sebacic acid G2 and adenosine H10 were withdrawn from this analysis due to their unclear results; water A1 was used to normalize all OD data) are reported. The $93 \times 6 = 558$ growth curves have been clustered into three categories: large, medium, and small.

Data that gave rise to Figure 2 were used to construct a contingency table (Table 1) where, within each category, substrates have been grouped according to the isolates that metabolize them (Table 1). Data presented in Table 1 indicate that, among *Fusarium* isolates, *F. graminearum* (55, 23, and 15 substrates supporting large, medium, and small growth, respectively) had the best catabolic versatility, followed by *F. culmorum* (7, 51, and 35 substrates supporting large, medium, and small growth, respectively) and *F. oxysporum* (1, 59, and 33 substrates supporting large, medium, and small growth, respectively). In detail, *F. graminearum* showed the best saprotrophic ability, whereas *F. culmorum* grew fast on seven substrates, five of which are in common with *F. graminearum*, that is, quinic acid (F12), L-alanine (G8), L-asparagine (G10), L-aspartic acid (G11), and L-glutamic acid (G12). The only substrate where *F. oxysporum* grew

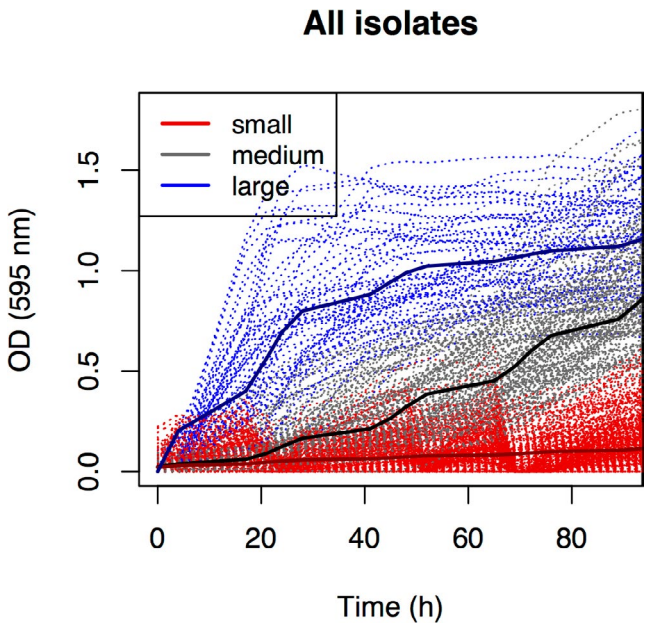

FIGURE 2 Exploratory clustering of optical density (OD) growth curves into groups corresponding to growth features: growth curves of OD data for each isolate and substrate are projected onto adequate basis and curve clusters are found by semiparametric *k*-centres functional clustering. Each substrate is classified as large (fast growth, blue line), medium (medium growth, grey-black line), or small (poor growth, red line) [Colour figure can be viewed at wileyonlinelibrary.com]

fast is L-asparagine (G10), in common with both *F. graminearum* and *F. culmorum*.

With respect to *T. gamsii* T6085 (0, 29, and 64 substrates supporting large, medium, and small growth, respectively), the antagonistic isolate collocated in an intermediate position. However, among those substrates supporting medium growth, D-cellobiose (A12), α-D-glucose (B12), and glycogen (C5) are in common with all the *Fusarium* isolates that had medium ability to metabolize such substrates. Finally, both *F. langsethiae* and *F. sporotrichioides* showed a very slow growth rate on all substrates, with their profiles characterized only by substrates supporting small growth.

3.2 | Assessment – Bayesian generalized additive models

The first step of this second analysis was to obtain the "best" estimate of each growth curve for each isolate. Then, the behaviour of each isolate in each substrate was assessed by an inferential procedure that allows a probabilistic comparison among isolates within substrates and the assignment of a score to each isolate valid for comparison within each substrate. Growth scores, defined by uncertainty measures, are shown in Table 2. Substrates included in the Biolog PM FF microplates were ordered according to Atanasova and Druzhinina (2010), as follows: 1 = monosaccharides (1.1 heptoses, 1.2 hexoses, 1.3 pentoses); 2 = monosaccharide-related compounds (2.1 sugar acids, 2.2 hexosamines, 2.3 polyols); 3 = other sugars (3.1 polysaccharides, 3.2 oligosaccharides, 3.3 glucosides); 4 = nitrogen-containing compounds (4.1 peptides, 4.2 L-amino acids, 4.3 biogene and heterocyclic amines, 4.4 TCA cycle intermediates, 4.5 aliphatic organic acids); 5 = others.

Cells in Table 2 are marked with different colours according to their values, varying from 1.25 (blue) to −0.086 (red), to give a visual assessment of the different catabolic activity of the four pathogens, *T. gamsii* T6085, and *F. oxysporum*. The column for *F. graminearum* scores shows the highest number of blue cells (Table 2). According to score values, *F. graminearum* was able to grow the best on the majority of the tested substrates (74 out of 93 substrates), followed by *T. gamsii* T6085, *F. culmorum*, and *F. oxysporum*, that showed similar behaviour, showing the highest scores when grown on six, five, and four out of the 93 substrates, respectively. However, *F. graminearum* generally had a good catabolic versatility, showing an average score of 1.012, whereas *F. culmorum*, *T. gamsii* T6085, and *F. oxysporum* had an average score of 0.479, 0.334, and 0.513, respectively. Also, in this second analysis, *F. langsethiae* and *F. sporotrichioides* were confirmed to have a scarce ability to grow on different substrates because they showed, in both cases, a score value of 0.188. Despite the ability of *F. graminearum* to grow well on the majority of the substrates, from Table 2 it is also possible to appreciate differences between its catabolic capacity and that of the nonpathogenic isolates *T. gamsii* T6085 and the natural competitor *F. oxysporum* for specific substrates, with sugars apparently playing an important role. For example, within the group of polysaccharides (3.1), α- and β-cyclodextrin (B1 and B2, respectively) were poorly assimilated by *F. graminearum* (score = 0.166 and = 0.046, respectively), whereas *T. gamsii* was able to catabolize B1 (score = 1.230) and *F. oxysporum* could catabolize B2 (score = 1.156).

Among oligosaccharides (3.2), the pathogen seemed unable to catabolize C10 (maltitol), showing a score of 0.193, while *T. gamsii* grew very well, with a score of 0.817. Two other oligosaccharides, C8 (α-D-lactose) and C9 (lactulose), were assimilated well by *T. gamsii* T6085 (both scores around 1.000), while the pathogen did not show a good catabolic ability when inoculated on them (scores = 0.477 and 0.134, respectively). Among monosaccharide-related compounds, the sugar acid D-galacturonic acid (B8) was scarcely catabolized by the pathogen (score = 0.342) whereas *F. oxysporum* seemed to use it well (score = 1.022).

Finally, among monosaccharides, *F. graminearum* could not grow well on the pentose D-arabinose (A8), showing a score of 0.186, whereas *F. oxysporum* showed a score of 1.014. The pathogen grew on its stereoisomer L-arabinose (A9), showing a score of 0.655, comparable with that of *F. oxysporum*. The six isolates were ranked on each substrate and then the frequency distribution of ranks was obtained for each isolate (Table 3). *F. graminearum* showed the highest frequency for rank 1 (76 out of 93), followed by *T. gamsii* T6085 (7), and *F. oxysporum* and *F. culmorum* with very similar values (6 and 4, respectively). However, *T. gamsii* T6085 was positioned at rank 6 for a quarter of the substrates. Finally, *F. langsethiae* and *F. sporotrichioides* showed a very high frequency distribution for rank 5 (33 and 32,

TABLE 1 Substrates included in the Biolog phenotype microarray FF microplates grouped by semiparametric functional clustering according to their ability to be metabolized by each isolate

Isolate	Small	Medium	Large
Fusarium culmorum	A2 A3 A4 A8 B1 B2 B4 B6 B8 B11 C2 C4 C6 C8 C9 C10 D1 D2 D6 D7 D10 D12 E3 E8 F2 F5 F6 F7 F8 G6 G7 G9 H1 H8 H12	A5 A6 A7 A9 A10 A11 A12 B3 B5 B7 B9 B10 B12 C1 C3 C5 C7 C11 C12 D3 D4 D5 D9 D11 E1 E2 E4 E5 E6 E7 E9 E10 E11 E12 F1 F3 F4 F9 F10 F11 G1 G3 G4 G5 H2 H4 H5 H6 H7 H9 H11	D8 F12 G8 G10 G11 G12 H3
Fusarium graminearum	A3 A8 B1 B2 B6 B8 C1 C2 C8 C9 C10 D6 D10 E3 F6	A2 A5 A9 A12 B4 B7 B9 B11 B12 C5 C6 D2 D7 D9 D12 E1 F2 F8 G3 G6 H3 H5 H8	A4 A6 A7 A10 A11 B3 B5 B10 C3 C4 C7 C11 C12 D1 D3 D4 D5 D8 D11 E2 E4 E5 E6 E7 E8 E9 E10 E11 E12 F1 F3 F4 F5 F7 F9 F10 F11 F12 G1 G4 G5 G7 G8 G9 G10 G11 G12 H1 H2 H4 H6 H7 H9 H11 H12
Fusarium langsethiae	A2 A3 A4 A5 A6 A7 A8 A9 A10 A11 A12 B1 B2 B3 B4 B5 B6 B7 B8 B9 B10 B11 B12 C1 C2 C3 C4 C5 C6 C7 C8 C9 C10 C11 C12 D1 D2 D3 D4 D5 D6 D7 D8 D9 D10 D11 D12 E1 E2 E3 E4 E5 E6 E7 E8 E9 E10 E11 E12 F1 F2 F3 F4 F5 F6 F7 F8 F9 F10 F11 F12 G1 G3 G4 G5 G6 G7 G8 G9 G10 G11 G12 H1 H2 H3 H4 H5 H6 H7 H8 H9 H11 H12		
Fusarium oxysporum	A3 A5 A6 B1 B2 B4 B6 B8 B11 C1 C2 C6 C8 C9 C10 D6 D7 D10 E2 E3 E8 F2 F5 F7 F8 G6 G7 H1 H3 H7 H11 H12	A2 A4 A7 A8 A9 A10 A11 A12 B3 B5 B7 B9 B10 B12 C3 C4 C5 C7 C11 C12 D1 D2 D3 D4 D5 D8 D9 D11 D12 E1 E4 E5 E6 E7 E9 E10 E11 E12 F1 F3 F4 F6 F9 F10 F11 F12 G1 G3 G4 G5 G8 G9 G11 G12 H2 H4 H5 H6 H8 H9	G10
Fusarium sporotrichioides	A2 A3 A4 A5 A6 A7 A8 A9 A10 A11 A12 B1 B2 B3 B4 B5 B6 B7 B8 B9 B10 B11 B12 C1 C2 C3 C4 C5 C6 C7 C8 C9 C10 C11 C12 D1 D2 D3 D4 D5 D6 D7 D8 D9 D10 D11 D12 E1 E2 E3 E4 E5 E6 E7 E8 E9 E10 E11 E12 F1 F2 F3 F4 F5 F6 F7 F8 F9 F10 F11 F12 G1 G3 G4 G5 G6 G7 G8 G9 G10 G11 G12 H1 H2 H3 H4 H5 H6 H7 H8 H9 H11 H12		
Trichoderma gamsii T6085	A3 A4 A5 A8 A9 B1 B2 B6 B8 B10 B11 C1 C2 C3 C4 C6 C7 C9 C10 C11 D3 D5 D6 D7 D8 D9 D10 D12 E1 E3 E4 E5 E8 E11 F1 F2 F3 F4 F5 F6 F7 F8 F9 F10 F11 F12 G1 G3 G4 G5 G6 G7 G9 H1 H2 H3 H4 H5 H6 H7 H8 H9 H11 H12	A2 A6 A7 A10 A11 A12 B3 B4 B5 B7 B9 B12 C5 C8 C12 D1 D2 D4 D11 E2 E6 E7 E9 E10 E12 G8 G10 G11 G12	

Abbreviations: Small, poor growth; medium, medium growth; large, fast growth.

respectively) and rank 6 (30 and 31, respectively), corresponding to approximately a third of the substrates.

4 | DISCUSSION

Within the scenario of a complex disease such as FHB of wheat, knowledge of the nutrient requirements of the main causal agents and potential biocontrol agents is a fundamental prerequisite in order to define the best strategy for disease management (Sarrocco & Vannacci, 2018). In this context, substrate colonization is the first step in the cascade of events that lead to the use of different biological control mechanisms such as antibiosis, mycoparasitism, and induction of resistance in host plants (Jaroszuk-Scise et al., 2019). The knowledge of comparative nutritional requirements among the main actors of debris colonization (either natural or deliberately

TABLE 2 Growth scores, defined by uncertainty measures, assigned to each isolate for each substrate included in the Biolog phenotype microarray FF microplates

Well	FG	TG	FC	FL	FS	FO	Substrate	Group
E3	0.813	0.762	0.812	0.456	0.778	0.706	Sedoheptulosan	1.1
B12	1.030	0.818	0.579	0.261	0.242	0.878	α-D-Glucose	1.2
B5	0.998	0.644	0.275	0.082	0.004	0.335	D-Fructose	1.2
B7	0.958	0.693	0.314	0.109	−0.078	0.705	D-Galactose	1.2
D2	0.902	0.936	0.434	0.206	0.214	0.678	D-Mannose	1.2
E8	1.079	0.231	0.253	0.287	0.251	0.156	D-Tagatose	1.2
B6	1.163	0.186	0.314	0.157	0.238	0.453	L-Fucose	1.2
D12	0.991	0.113	0.248	0.190	0.194	0.573	L-Rhamnose	1.2
E5	1.146	0.309	0.338	0.312	0.180	0.672	L-Sorbose	1.2
A8	0.186	0.120	0.245	0.157	0.272	1.014	D-Arabinose	1.3
D10	1.216	0.172	0.303	0.176	0.185	0.299	D-Psicose	1.3
E1	0.855	0.081	0.965	0.046	0.161	0.937	D-Ribose	1.3
E12	1.087	0.657	0.790	0.315	0.173	0.686	D-Xylose	1.3
A9	0.655	0.060	0.833	0.051	0.178	0.919	L-Arabinose	1.3
C7	1.229	0.059	0.437	0.038	−0.011	0.630	2-Keto-D-gluconic acid	2.1
B8	0.342	0.100	0.643	0.199	0.187	1.022	D-Galacturonic acid	2.1
B10	1.187	0.155	0.460	0.131	0.117	0.521	D-Gluconic acid	2.1
C3	1.210	0.102	0.510	0.027	−0.051	0.604	D-Glucuronic acid	2.1
G1	1.190	0.159	0.553	0.128	0.089	0.571	D-Saccharic acid	2.1
C2	1.169	0.110	0.325	0.139	0.142	0.177	Glucuronamide	2.1
B11	1.067	0.065	0.166	0.002	−0.001	0.501	D-Glucosamine	2.2
A3	0.623	0.998	0.205	0.083	0.203	0.127	N-Acetyl-D-galactosamine	2.2
A4	1.172	0.142	0.147	0.130	0.165	0.801	N-Acetyl-D-glucosamine	2.2
A5	0.630	0.208	1.022	0.053	0.159	0.133	N-Acetyl-D-mannosamine	2.2
A6	1.213	0.446	0.359	0.092	0.148	0.127	Adonitol	2.3
A10	1.174	0.574	0.268	0.131	0.200	0.741	D-Arabitol	2.3
D1	1.229	0.676	0.278	0.100	0.064	0.502	D-Mannitol	2.3
E4	1.167	0.157	0.596	0.269	0.238	0.694	D-Sorbitol	2.3
C4	1.219	0.028	0.219	0.092	0.047	0.284	Glycerol	2.3
B4	1.249	0.549	0.188	0.081	0.069	0.066	*i*-Erythritol	2.3
C6	1.026	0.119	0.355	0.007	−0.026	0.683	*m*-Inositol	2.3
E11	1.153	0.200	0.488	0.241	0.258	0.555	Xylitol	2.3
B1	0.166	1.230	0.353	0.166	0.138	0.540	α-Cyclodextrin	3.1
B2	0.046	0.240	0.735	0.148	0.025	1.156	β-Cyclodextrin	3.1
B3	0.987	0.671	0.798	0.282	0.345	0.550	Dextrin	3.1
C5	0.887	0.991	0.786	0.279	0.525	0.714	Glycogen	3.1
C8	0.477	1.028	0.230	0.209	0.215	0.102	α-D-Lactose	3.2
A12	1.088	0.809	0.431	0.269	0.275	0.802	D-Cellobiose	3.2
D3	1.158	0.081	0.521	0.219	0.065	0.417	D-Melezitose	3.2
D4	1.171	0.339	0.372	0.098	0.135	0.509	D-Melibiose	3.2
D11	1.220	0.147	0.695	0.234	0.215	0.603	D-Raffinose	3.2
B9	1.139	0.565	0.371	0.105	0.130	0.555	Gentiobiose	3.2
C9	0.134	1.011	0.237	0.141	0.243	0.225	Lactulose	3.2
C10	0.193	0.817	0.460	0.175	0.378	0.282	Maltitol	3.2
C11	1.209	0.122	0.304	0.249	0.242	0.613	Maltose	3.2

(Continues)

TABLE 2 (Continued)

Well	FG	TG	FC	FL	FS	FO	Substrate	Group
C12	1.197	0.444	0.495	0.237	0.262	0.728	Maltotriose	3.2
D9	1.219	0.121	0.603	0.210	0.062	0.584	Palatinose	3.2
D5	1.225	0.209	0.488	0.078	0.062	0.632	α-Methyl-D-galactoside	3.3
D7	1.236	0.093	0.273	0.199	0.094	0.188	α-Methyl-D-glucoside	3.3
A7	1.227	0.433	0.353	0.036	0.143	0.702	Amygdalin	3.3
A11	1.098	0.361	0.344	0.248	0.313	0.420	Arbutin	3.3
D6	0.441	0.092	0.225	0.067	0.201	1.031	β-Methyl-D-galactoside	3.3
D8	1.194	0.200	0.790	0.097	0.196	0.495	β-Methyl-D-glucoside	3.3
E9	1.085	0.599	0.614	0.221	0.139	0.491	D-Trehalose	3.3
E2	1.229	0.393	0.544	0.305	0.139	0.209	Salicin	3.3
E6	1.187	0.352	0.620	0.283	0.270	0.485	Stachyose	3.3
E7	1.072	0.631	0.615	0.283	0.379	0.478	Sucrose	3.3
E10	1.112	0.620	0.531	0.278	0.238	0.713	Turanose	3.3
H1	1.018	0.137	0.142	0.215	0.114	0.107	Glycyl-L-glutamic acid	4.1
G9	1.177	0.271	0.275	0.272	0.286	0.463	L-Alanyl-glycine	4.1
F1	1.138	0.031	0.422	0.220	0.093	0.719	γ-Aminobutyric acid	4.2
G8	1.057	0.218	0.689	0.269	0.259	0.611	L-Alanine	4.2
G10	1.091	0.391	0.845	0.184	0.297	0.577	L-Asparagine	4.2
G11	1.071	0.352	0.661	0.331	0.398	0.616	L-Aspartic acid	4.2
G12	1.071	0.349	0.650	0.341	0.243	0.596	L-Glutamic acid	4.2
H2	1.174	0.159	0.286	0.272	0.258	0.658	L-Ornithine	4.2
H3	0.982	0.136	1.121	0.263	0.222	0.086	L-Phenylalanine	4.2
H4	1.125	0.142	0.642	0.272	0.260	0.627	L-Proline	4.2
H5	0.992	0.462	0.969	0.265	0.251	0.864	L-Pyroglutamic acid	4.2
H6	1.013	0.371	0.629	0.360	0.280	0.633	L-Serine	4.2
H7	0.984	0.135	0.478	0.197	0.100	0.109	L-Threonine	4.2
G6	0.897	0.225	0.154	0.334	0.306	0.222	N-Acetyl-L-glutamic acid	4.2
H8	1.153	0.466	0.621	0.234	0.319	0.918	2-Amino ethanol	4.3
H9	1.109	0.126	0.882	0.214	0.241	0.569	Putrescine	4.3
H11	1.007	0.145	0.221	0.211	0.096	0.102	Uridine	4.3
F7	1.239	0.202	0.269	0.170	0.197	0.365	α-Ketoglutaric acid	4.4
F10	1.204	0.052	0.380	0.131	0.137	0.239	D-Malic acid	4.4
F3	1.243	0.166	0.555	0.109	0.125	0.361	Fumaric acid	4.4
F11	1.231	0.237	0.469	0.165	0.086	0.424	L-Malic acid	4.4
G4	1.185	0.230	0.533	0.264	0.111	0.419	Succinic acid	4.4
F4	1.215	0.098	0.343	0.134	0.189	0.463	β-Hydroxybutyric acid	4.5
F2	1.151	0.096	0.491	0.046	0.227	0.172	Bromosuccinic acid	4.5
F5	1.250	0.208	0.291	0.183	0.193	0.296	γ-Hydroxybutyric acid	4.5
F9	1.197	0.067	0.422	0.139	0.131	0.348	L-Lactic acid	4.5
H12	0.999	0.153	0.143	0.236	0.146	0.141	Adenosine-5′-monophosphate	5
F8	1.220	0.134	0.202	0.162	0.169	0.250	D-Lactic acid methyl ester	5
C1	0.430	0.408	1.049	0.135	−0.005	−0.086	Glucose-1-phosphate	5
G7	1.026	0.151	0.134	0.252	0.154	0.159	L-Alaninamide	5
F6	0.549	0.158	0.487	0.076	0.295	1.112	*p*-Hydroxyphenylacetic acid	5
F12	1.208	0.191	0.544	0.267	0.252	0.444	Quinic acid	5

(Continues)

TABLE 2 (Continued)

Well	FG	TG	FC	FL	FS	FO	Substrate	Group
G3	0.863	0.127	0.757	0.218	0.196	0.720	Succinamic acid	5
G5	1.171	0.201	0.573	0.250	0.245	0.615	Succinic acid monomethyl ester	5
A2	0.939	0.802	0.522	0.245	0.157	0.822	Tween 80	5

Note: The red to blue colour scale corresponds to increasing values of the growth scores. Carbon substrates found in the FF plates ordered according to the groups proposed by Atanasova and Druzhinina (2010): 1: monosaccharides: 1.1 heptoses, 1.2 hexoses, 1.3 pentoses; 2: monosaccharide-related compounds: 2.1 sugar acids, 2.2 hexosamines, 2.3 polyols; 3: other sugars: 3.1 polysaccharides, 3.2 oligosaccharides, 3.3 glucosides; 4: nitrogen-containing compounds: 4.1 peptides, 4.2 L-amino acids, 4.3 biogene and heterocyclic amines, 4.4 TCA-cycle intermediates, 4.5 aliphatic organic acids; 5: others.

Abbreviations: FG, *Fusarium graminearum*; TG, *Trichoderma gamsii* T6085; FC, *Fusarium culmorum*; FL, *Fusarium langsethiae*; FS, *Fusarium sporotrichioides*; FO, *Fusarium oxysporum*.

TABLE 3 Frequency distribution of ranks and isolates for all substrates

	Isolate						
Rank	FG	TG	FC	FL	FS	FO	Total
1	76	7	4	0	0	6	93
2	9	7	34	5	2	36	93
3	3	14	38	4	6	28	93
4	2	26	14	21	22	8	93
5	2	16	1	33	32	9	93
6	1	23	2	30	31	6	93
Total	93	93	93	93	93	93	

Abbreviations: FG, *Fusarium graminearum*; TG, *Trichoderma gamsii* T6085; FC, *Fusarium culmorum*; FL, *Fusarium langsethiae*; FS, *Fusarium sporotrichioides*; FO, *Fusarium oxysporum*.

introduced) can help to rank nutrient competition as one of the major (or minor, as seems to be the case) mechanisms of action of a successful antagonist. As a side effect, comparative nutritional analysis offers the opportunity to identify nutrients solely exploited by the antagonist, suggesting the combined use of the antagonist and such nutrient(s) in field applications could offer an ecological advantage to the beneficial fungus.

F. graminearum and *F. culmorum* are recognized worldwide as the main causal agents of FHB whereas, more recently, *F. langsethiae* has been frequently isolated from wheat kernels in Europe. There has been significant interest in the latter pathogen, together with *F. sporotrichioides*, due to their quite new mycotoxigenic arsenal (Nazari et al., 2019). These four pathogens were chosen in the present work, together with the beneficial isolate *T. gamsii* T6085 (Matarese et al., 2012; Sarrocco et al., 2019, 2020; Vicente et al., 2020), studied for its potential as a biocontrol agent of FHB, and *F. oxysporum* 7,121 (Sarrocco et al., 2012), well known for its ability to compete for cultural debris, as model organisms for setting up a new statistical protocol to better exploit data derived by the PM system and therefore to fully understand their catabolic ability in the perspective of biological control of FHB on wheat.

Because it is generally accepted that fungal phenotype is mainly determined by macronutrients that could act as territory for competition, the availability of a system that includes the maximum number of nutrients in a single assay would be an ideal tool to measure the metabolic diversity of these organisms. It is not easy to imagine a single assay that allows the simultaneous testing of hundreds of carbon and nitrogen sources, as well as sulphur and phosphorus ones, and also including several important environmental conditions such as pH, light, and oxygen availability (Atanasova et al., 2010). However, the Biolog PM system seems to be capable of doing this, providing a phenotypic characterization of several fungal isolates in a short time.

Although it is accepted that the PM system can be used to obtain information on the catabolic phenotypes of fungi, both at isolate and community level (Bochner et al., 2011), much more controversial and complex is the issue of data analysis. Analytical methods used and developed until now have been extensively reviewed by Pinzari et al. (2016). However, even if complex approaches such as kinetic or multivariate analysis are described, single time-point estimation is still the most frequently used tool for elaborating this kind of data (Oszust et al., 2020). The protocol adopted in the present study can be applied to two or more fungi that require comparison according to their nutritional requirements. A very promising field of application is the study of synthetic microbial consortia (Kong et al., 2018), where single components should occupy different ecological niches to avoid possible competition among members of the consortium, but must share at least part of their nutritional requirements with the pathogen, to boost competition for resources and restrict or suppress its activity (Niu et al., 2020).

The statistical protocol set up in the present work can be used in two different ways. Using the functional principal component analysis, it is possible to effectively describe global features of isolates, determine their general preferences in terms of substrate, and envisage similarities in terms of growth. Based on functional principal component analysis, the characterization approach allows for adaptive estimation of growth curves but prevents a proper uncertainty assessment. Relying on the Bayesian GAMs instead, it is possible to rigorously compare growth behaviours in terms of specific growth parameters, and rank isolates in terms of summary scores, accounting for estimation uncertainty. In summary, functional principal

component analysis has higher flexibility in describing similarity patterns of growth curves, while Bayesian GAMs, and the subsequent computation of growth parameters, allow inferences on specific growth features. Both approaches involve the semiparametric estimation of growth curves and are complementary and comparable in terms of computational complexity.

Results obtained by the functional clustering presented here gave a general overview of the different behaviour of the four pathogens and the two nonpathogenic isolates. From this analysis, *F. graminearum* seemed to potentially be the most competitive isolate in terms of nutrient assimilation, being able to quickly grow on the majority of tested substrates. This is in agreement with Leplat et al. (2012) that, among all *Fusarium* species involved in the FHB of wheat, *F. graminearum* is a good saprotroph thanks to its wide enzymatic arsenal that allows a rapid growth when fresh matter is available. Data shown in Table 2 can be of further help in choosing substrates that could put the nonpathogenic isolate at a competitive advantage towards *F. graminearum*.

From our analysis, *F. culmorum* was the second isolate, in order of growth rate, as it developed fast on seven substrates, six of which were in common with *F. graminearum*. This apparent niche overlap supports Xu and Nicholson's (2009) explanation when describing the community ecology of fungal pathogens causing FHB. Disease development is the result of the interactions of pathogen components, where *F. graminearum* is the most competitive, while the competitiveness of *F. culmorum* varies with the competing species (Xu & Nicholson, 2009). *T. gamsii* T6085 and *F. oxysporum* 7,121 seemed to occupy an intermediate position, thus confirming on the one hand the metabolic versatility of *Trichoderma* species to adapt to several environments (Kubicek et al., 2019), and on the other hand, the potential nutritional competitive ability of isolates belonging to *F. oxysporum* species that are well known to have a saprotrophic capacity, allowing them to outcompete other organisms on natural substrates such as crop residues (Sarrocco et al., 2019).

The other two pathogens, *F. langsethiae* and *F. sporotrichioides*, were functionally clustered in the small category, because they were never able to grow fast on any of the substrates included in the FF microplates. This appears to be in contrast with what has been reported in the literature, where *F. sporotrichioides* is described as one of the other *Fusarium* species associated with FHB that show a better saprotrophic capacity in soil than *F. graminearum* (Pereyra and Dill-Macky, 2008).

Information collected by the second analysis here gave a statistically supported comparison of the catabolic ability of each isolate. Scores calculated here allow for a better appreciation and comparison of the behaviour of the six fungi on each substrate. This approach also gives a tool to rapidly detect how many and which substrates are differentially used. The first evident difference in the catabolic ability of *F. graminearum* and *T. gamsii* T6085 can be found for α-cyclodextrin, which was well used by the antagonist and scarcely exploited by the pathogen. Oros et al. (2020) published an investigation of the growth and development of 17 *Trichoderma* species on α- and β-cyclodextrin, in order to evaluate the possibility of using this substrate for formulation of biologically active chemicals in solid state dispersion and liquid state. The authors indicated that *Trichoderma* species preferred the α- and γ-cyclodextrin to β-cyclodextrin, which is in line with what we observed in the *T. gamsii* isolate here that grew well on α-cyclodextrin and poorly on β-cyclodextrin. In addition, they suggested that this information may contribute to promote the elimination of this class of compounds from any organic and inorganic matrices (Oros et al., 2020). At the same time, the scarce growth of *F. graminearum* and the other pathogenic *Fusarium* spp. on both α- and β-cyclodextrin may be of particular relevance in view of the control of these pathogens, because this compound is already used with tebuconazole for the management of foot and crown rot of wheat caused by *F. culmorum* (Balmas et al., 2006).

Another substrate differentially used by *F. graminearum* (slowly) and *T. gamsii* T6985 (rapidly) was maltitol. The assimilation of this specific polyol, already observed in several *Trichoderma* spp., may have a role on the ecology of *T. gamsii* T6085, because it could be used as an indicator of dehydrogenase activity potentially involved in survival when drought conditions occur (Hoyos-Carvajal & Bissett, 2011).

More difficult to explain is the different behaviour of *T. gamsii* T6085 and *F. graminearum* on both α-D-lactose and lactulose. This is especially due to the fact that metabolism of both these substrates is involved in the intracellular galactoglycome in *Trichoderma reesei* for the production of cellulases and hemicellulases (Karaffa et al., 2013).

Even if referring to a narrow group of isolates, this work shows a new protocol for the analysis of data collected by the PM system, allowing full exploitation of data obtained by this phenotypic approach and, at the same time, providing ecological information about what one isolate prefers compared to the others. Many other diseases rely on plant debris colonization by the pathogen(s) to guarantee their survival, and residue conservation increases the risk of epidemics for cereal, and specifically wheat, diseases (Kerdraon et al., 2019). In the context of a biological control strategy, these substrates (preferred by the antagonist and not by the pathogens) could be evaluated as additives to *Trichoderma* biopreparations in order to improve competitiveness in the targeted pathogen community (Oszust et al., 2020). However, it is fundamental to keep in mind that substrate competition is only a part of a much more complex interaction occurring among organisms that involves many other environmental factors, such as temperature, pH, water availability, as well as other mechanisms based on the physical and chemical interactions among competitors, as has been demonstrated for *T. gamsii* T6085 (Sarrocco et al., 2019).

CONFLICT OF INTEREST

None of the authors have present or potential conflicts of interest, nor financial, personal, or other relationships with other persons or organizations that might inappropriately influence or be perceived to influence their work.

DATA AVAILABILITY STATEMENT

The data that support the findings of this study are available from the corresponding author upon reasonable request.

ORCID

Giovanna Jona Lasinio https://orcid.org/0000-0001-8912-5018
Alessio Pollice https://orcid.org/0000-0002-2818-9373
Livia Pappalettere https://orcid.org/0000-0002-8803-3557
Giovanni Vannacci https://orcid.org/0000-0001-8218-6029
Sabrina Sarrocco https://orcid.org/0000-0002-7080-8369

REFERENCES

Atanasova, L. & Druzhinina, I.S. (2010) Global nutrient profiling by phenotype MicroArrays: a tool complementing genomic and proteomic studies in conidial fungi. *Journal of Zhejiang University Science B*, *11*, 151–168.

Balmas, V., Delogu, G., Sposito, S., Rau, D. & Migheli, Q. (2006) Use of a complexation of tebuconazole with β-cyclodextrin for controlling foot and crown rot of durum wheat incited by *Fusarium culmorum*. *Journal of Agricultural and Food Chemistry*, *54*, 480–484.

Baroncelli, R., Zapparata, A., Piaggeschi, G., Sarrocco, S. & Vannacci, G. (2016) Draft whole-genome sequence of *Trichoderma gamsii* T6085, a promising biocontrol agent of Fusarium head blight on wheat. *Genome Announcements*, *4*, e01747-15.

Bochner, B.R., Gadzinski, P. & Panomitros, E. (2011) Phenotype microArrays for high-throughput phenotypic testing and assay of gene function. *Genome Resources*, *11*, 1246–1255.

Brooker, R.W., Callaway, R.M., Cavieres, L.A., Kikvidze, Z., Lortie, C., Michalet, R. et al. (2009) Don't diss integration: a comment on Ricklefs's disintegrating communities. *The American Naturalist*, *174*, 919–927.

Chiou, J.M. & Li, P.L. (2007) Functional clustering and identifying substructures of longitudinal data. *Journal of the Royal Statistical Society: Series B*, *69*, 679–699.

Fitt, B.D., Huang, Y.J., van den Bosch, F. & West, J.S. (2006) Coexistence of related pathogen species on arable crops in space and time. *Annual Review of Phytopathology*, *44*, 163–182.

Holomuzki, J.R., Feminella, J.W. & Power, M.E. (2010) Biotic interactions in freshwater benthic habitats. *Journal of the North American Benthological Society*, *29*, 220–244.

Hoyos-Carvajal, L. & Bissett, J. (2011) Biodiversity of *Trichoderma* in Neotropics. In: Grillo, O. and Venora, G. (Eds.) *The Dynamical Processes of Biodiversity – Case Studies of Evolution and Spatial Distribution*. InTech, pp. 303–320.

Jaroszuk-Scise, J., Tyskiewicz, R., Nowak, A., Ozimek, E., Majewska, M., Hanaka, A. et al. (2019) Phytohormones (auxin, gibberellin) and ACC deaminase in vitro synthesized by the mycoparasitic *Trichoderma* DEMTkZ3A0 strain and changes in the level of auxin and plant resistance markers in wheat seedlings inoculated with this strain conidia. *International Journal of Molecular Sciences*, *20*, 4923.

Karaffa, L., Coulier, L., Fekete, E., Overkamp, K.M., Druzhinina, I.S., Mikus, M. et al. (2013) The intracellular galactoglycome in *Trichoderma reesei* during growth on lactose. *Applied Microbial Biotechnology*, *97*, 5447–5456.

Kerdraon, L., Laval, V. & Suffert, F. (2019) Microbiomes and pathogen survival in crop residues, an ecotone between plant and soil. *Phytobiomes Journal*, *3*, 246–255.

Kinkel, L., Schlatter, D., Xiao, K. & Baines, A.D. (2014) Sympatric inhibition and niche differentiation suggest alternative coevolutionary trajectories among *Streptomycetes*. *ISME Journal*, *8*, 249–256.

Kong, Z., Hart, M. & Hongguang, L. (2018) Paving the way from the lab to the field: using synthetic microbial consortia to produce high-quality crop. *Frontiers in Plant Science*, *9*, 1467.

Kubicek, C.P., Steindorff, A.S., Chenthamara, K., Manganiello, G., Henrissat, B., Zhang, J. et al. (2019) Evolution and comparative genomics of the most common *Trichoderma* species. *BMC Genomics*, *20*, 485.

Leplat, J., Friberg, H., Abid, M. & Steinberg, C. (2012) Survival of *Fusarium graminearum*, the causal agent of Fusarium head blight. A review. *Agronomy for Sustainable Development*, *33*, 97–111.

Matarese, F., Sarrocco, S., Gruber, S., Seidl-Seiboth, V. & Vannacci, G. (2012) Biocontrol of Fusarium head blight: interactions between *Trichoderma* and mycotoxigenic *Fusarium*. *Microbiology*, *158*, 98–106.

Nazari, L., Pattori, E., Somma, S., Manstretta, V., Waalwijk, C., Moretti, A. et al. (2019) Infection incidence, kernel colonisation, and mycotoxin accumulation in durum wheat inoculated with *Fusarium sporotrichioides*, *F. langsethiae* or *F. poae* at different growth stages. *European Journal Plant Pathology*, *153*, 715–729.

Niu, B., Wang, W., Yuan, Z., Sederoff, R.R., Sederoff, H., Chiang, V.L. et al. (2020) Microbial interactions within multiple-strain biological control agents impact soil-borne plant disease. *Frontiers in Microbiology*, *11*, 2452.

Oros, G., Jakab, A. & Cserhati, T. (2020) Utilization of cyclodextrins by *Trichoderma* species. *Open Chemical and Biomedical Methods Journal*, *3*, 90–97.

Oszust, K., Cybulska, J. & Frąc, M. (2020) How do *Trichoderma* genus fungi win a nutritional competition battle against soft fruit pathogens? A report on niche overlap nutritional potentiates. *International Journal Molecular Science*, *21*, 4235.

Pereyra, S.A. & Dill-Macky, R. (2008) Colonization of the residues of diverse plant species by *Gibberella zeae* and their contribution to Fusarium head blight inoculum. *Plant Disease*, *92*, 800–807.

Pinzari, F., Ceci, A., Abu-Samra, N., Canfora, L., Maggi, O. & Persiani, A. (2016) Phenotype MicroArray™ system in the study of fungal functional diversity and catabolic versatility. *Research in Microbiology*, *167*, 710–722.

Sarrocco, S. (2016) Dung-inhabiting fungi: a potential reservoir of novel secondary metabolites for the control of plant pathogens. *Pest Management Science*, *72*, 643–652.

Sarrocco, S., Esteban, P., Vicente, I., Bernardi, R., Plainchamp, T., Domenichini, S. et al. (2020) Straw competition and wheat root endophytism of *Trichoderma gamsii* T6085 as useful traits in the biocontrol of Fusarium head blight. *Phytopathology*, https://doi.org/10.1094/PHYTO-09-20-0441-R

Sarrocco, S., Matarese, F., Moretti, A., Haidukowski, M. & Vannacci, G. (2012) DON on wheat crop residues: effects on mycobiota as a source of potential antagonists of *Fusarium culmorum*. *Phytopathologia Mediterranea*, *51*, 225–235.

Sarrocco, S., Valenti, F., Manfredini, S., Esteban, P., Bernardi, R., Puntoni, G. et al. (2019) Is exploitation competition involved in a multitrophic strategy for the biocontrol of Fusarium head blight? *Phytopathology*, *109*, 560–570.

Sarrocco, S. & Vannacci, G. (2018) Preharvest application of beneficial fungi as a strategy to prevent postharvest mycotoxin contamination: a review. *Crop Protection*, *110*, 160–170.

Scheipl, F., Fahrmeir, L. & Kneib, T. (2012) Spike-and-slab priors for function selection in structured additive regression models. *Journal of the American Statistical Association*, *107*, 1518–1532.

Torres, A.M., Palacios, S.A., Yerkovich, N., Palazzini, J.M., Battilani, P., Leslie, J.F. et al. (2019) Fusarium head blight and mycotoxins in wheat: prevention and control strategies across the food chain. *World Mycotoxins Journal*, *12*, 333–335.

Vaas, L.A.I., Sikorski, J., Michael, V., Goker, M. & Klenk, H.P. (2012) Visualization and curve-parameter estimation strategies for

efficient exploration of phenotype microarray kinetics. *PLoS One*, *7*, e34846.

Vicente, I., Baroncelli, R., Moran-Diez, M.E., Bernardi, R., Puntoni, G., Hermosa, R. et al. (2020) Combined comparative genomics and gene expression analyses provide insights into the terpene synthases inventory in *Trichoderma*. *Microorganisms*, *8*, 1603.

Wirsel, S.G., Runge-Frobose, C., Ahren, D.G.G., Kemen, E., Oliver, R.P. & Mendgen, K.W. (2002) Four or more species of *Cladosporium* sympatrically colonize *Phragmites australis*. *Fungal Genetics and Biology*, *35*, 99–113.

Xu, X. & Nicholson, P. (2009) Community ecology of fungal pathogens causing wheat head blight. *Annual Review of Phytopathology*, *47*, 83–103.

Yassouridis, C., Ernst, D. & Leisch, F. (2018) Generalization, combination and extension of functional clustering algorithms: the R package funcy. *Journal of Statistical Software*, *85*, 1–25.

Zapparata, A., Da Lio, D., Somma, S., Vicente Muñoz, I., Malfatti, L., Vannacci, G. et al. (2017) Genome sequence of *Fusarium graminearum* ITEM 124 (ATCC 56091), a mycotoxigenic plant pathogen. *Genome Announcements*, *5*, e01209-17.

How to cite this article: Lasinio GJ, Pollice A, Pappalettere L, Vannacci G, Sarrocco S. A statistical protocol to describe differences among nutrient utilization patterns of *Fusarium* spp. and *Trichoderma gamsii*. *Plant Pathol*. 2021;70:1146–1157. https://doi.org/10.1111/ppa.13362